BIOCHEMISTRY
including biophysical chemistry & molecular biology

Article

pubs.acs.org/biochemistry

Identification of Proximal and Distal Axial Ligands in *Leishmania major* Pseudoperoxidase

Rina Saha, Moumita Bose, Sumit Sen Santara, Jayasree Roy, and Subrata Adak*

Division of Structural Biology and Bio-informatics, CSIR-Indian Institute of Chemical Biology, 4, Raja S. C. Mullick Road, Kolkata 700 032, India

Supporting Information

ABSTRACT: Previous optical and electron paramagnetic resonance (EPR) spectroscopic studies of the newly discovered peroxynitrite scavenging pseudoperoxidase from *Leishmania major* (LmPP) suggested that ferric LmPP contained a six-coordinate low-spin (6cLS) heme with a thiolate ligand, presumably a cysteine, bound to its heme iron. To identify the axial ligands of LmPP, we exploit a systematic mutational analysis of potential heme ligands. On the basis of UV−visible and EPR spectroscopy, we report that the substitution of the proximal His206 with alanine in LmPP alters the 6cLS to a five-coordinate high spin (5cHS) form at pH 4.0 that has a spectrum characteristic of a Cys-ligated 5cHS derivative. The electronic absorption and EPR analysis of all alanine-substituted Cys and Met single mutants establish that when Cys107 is replaced with alanine, a new species appears that has a spectrum characteristic of a histidine-ligated 5cHS derivative at pH 4.0. Together, these results suggest that His206 and Cys107 act as the proximal and distal axial ligands in ferric LmPP, respectively. However, the electronic properties of reduced wild-type LmPP are similar to those of known 5cHS His-ligated heme proteins at pH 8.8, indicating that the thiolate bond was broken upon reduction. Furthermore, the wild-type protein was only partially reduced at pH 4.0, but the E105L mutant was completely reduced to form a 5cHS ferrous heme. These results imply that the presence of an acidic residue near the distal site may prevent reduction of the heme iron at acidic pH.

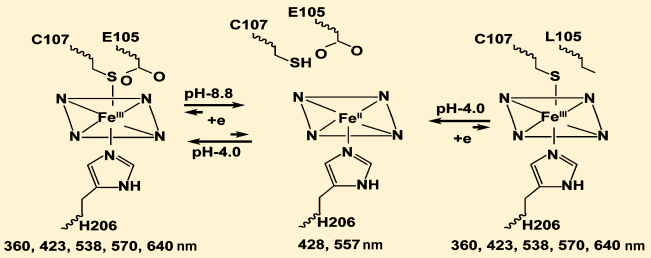

Heme proteins make up one of the most versatile classes of proteins in biology with respect to their functions, including oxygen transport and storage, peroxide/oxygen activation to oxygen insertion, active membrane transport, electron transfer, signal transduction, and control of gene expression.[1,2] The functional diversity and spectral characteristics of this class of proteins have mainly been attributed to the structural machinery of the protein environment that builds up the heme active site, especially the uniqueness of the proximal axial ligand and residues located in the distal pocket. Cytochromes, globins, heme oxygenases, and the majority of peroxidases employ a histidine residue as the proximal ligand in its protonated or deprotonated form.[3,4] Catalases utilize a tyrosine phenolate proximal axial ligand,[5] whereas a cysteine thiolate ligand is found in the cytochrome P450 (P450),[1] *Caldariomyces fumago* chloroperoxidase (CPO),[6] nitric oxide synthase,[7,8] cystathionine β-synthase (CBS),[9] and CO-sensing transcription factor (CooA) proteins.[10] Biochemical, spectroscopic, and X-ray crystallographic studies of wild-type and mutant enzymes have significantly contributed to our understanding of the structure−function aspects of heme proteins. Recently, site-directed mutagenesis has allowed researchers to determine the axial ligation of the heme proteins in different forms, e.g., ferric, ferrous, and ferrous CO forms of heme iron.

Among all the axial ligands identified for heme proteins to date, thiolate ligation through Cys has received the most attention. This type of ligation has been shown to be important to the reactivity and spectral characteristics of P450, NOS, CPO, CBS, and CooA.[1,8−10] The hemes in human CBS and CooA are 6cLS in both ferric and ferrous states.[10−12] Recent EPR, X-ray absorption,[9] and resonance Raman[13] spectroscopic characterization of the CBS has led to the assignment of the heme axial ligands as histidine and cysteine, respectively, in both oxidation states. Reduction of the heme results in retention of the thiolate ligand and a large red shift in the Soret peak to 450 nm. In contrast, reduction of CooA results in replacement of the thiolate ligand, Cys75, with a neighboring histidine residue, His77, and retention of the six-coordinate state with the Soret peak at 424 nm.[10,14] The recently determined crystal structure of CooA,[15] along with mutagenesis studies,[16] has revealed that the ligand *trans* to His77 in ferrous CooA is Pro2.

A novel type of pseudoperoxidase (LmPP) has been recently proposed to exhibit peroxynitrite degrading activities in the *Leishmania* parasite.[17] On the basis of homology modeling, its sequence is ∼14% identical and ∼40% conserved with the class I peroxidase, but it lacks a distal site His.[17,18] The other feature that distinguishes LmPP from peroxidase enzymes is the presence of a Cys205 residue in front of the proximal His206.

Received: July 12, 2013
Revised: November 20, 2013
Published: November 21, 2013

   dx.doi.org/10.1021/bi401343t | *Biochemistry* 2013, 52, 8878−8887

The optical and EPR spectra of LmPP are similar to those of both CBS and CooA, having thiolate-ligated 6cLS heme in ferric states.[17] Like those of CooA, the optical spectra of ferrous−CO complexes show the Soret absorption maxima at 420 nm. A possibility might be the replacement of proximal ligand Cys205 by a neighboring His206 residue during reduction.

Herein, we describe the spectroscopic characterization of the LmPP mutants (H206A, C205A, C205A/H206A, E105L, and C107A) in the Fe^{III}, Fe^{II}, and $Fe^{II}CO$ states using the techniques of electronic absorption. Our studies reveal that the two axial ligands in Fe^{III} LmPP are histidine 206 (not cysteine 205) at the proximal site and cysteine 107 at the distal site of the heme iron.

MATERIALS AND METHODS

Materials. Ni^{2+}-nitrilotriacetate resin and imidazole were obtained from Sigma-Aldrich. The sources of other reagents were described previously.[17,19,20] Peroxynitrite (Calbiochem, La Jolla, CA) was purchased as an aqueous solution (180−200 mM) and stored frozen at −80 °C until it was use. The stock solution was diluted with 0.005 M NaOH, and the peroxynitrite concentration was determined spectrophotometrically before each experiment by measuring the absorbance at 302 nm (ε_{302} = 1705 M^{-1} cm^{-1}).

Mutagenesis. Site-directed mutagenesis of LmPP DNA in the pET15B expression plasmid (encoding amino acids 48−346 and a six-His tag at the N-terminus) was performed using the QuikChange site-directed mutagenesis kit from Stratagene. Table S1 of the Supporting Information showed both sense and antisense primers for mutant proteins. The mutations were confirmed at the molecular biology core facility of the Indian Institute of Chemical Biology.

Protein Expression and Purification. Wild-type and mutant enzymes were overexpressed in *Escherichia coli* BL21 D3 and purified using Ni^{2+}-nitrilotriacetate affinity chromatography as reported previously.[17] After the crude extract had been loaded, the column was washed with washing buffer [50 mM phosphate buffer (pH 6.0) containing 0.1 mM ascorbate and 1 mM PMSF; 10 column volumes] and then washed further with 50 mM phosphate buffer (pH 5.25, 10 column volumes). The pure enzyme was eluted with 500 mM phosphate (pH 4.0) and then dialyzed three times against 50 mM phosphate (pH 4.0) to adjust from 500 to 50 mM phosphate. The purified enzyme was concentrated and stored at −80 °C. The heme was identified and quantified at pH 4.0 by the pyridine−hemochrome method.[17] Concentrations of C205A, E105L, and wild-type LmPP were determined from the 423 nm absorbance of the heme, using extinction coefficients of 71, 75, and 69 mM^{-1} cm^{-1}, respectively. Concentrations of C205A/H206A and H206A were determined from the absorbance at 382 nm of the heme, using extinction coefficients of 93 and 89 mM^{-1} cm^{-1}, respectively. The concentration of C107A was determined from the 408 nm absorbance of the heme, using an extinction coefficient of 89 mM^{-1} cm^{-1}.

Peroxynitrite Scavenging Activity Measurement. The rate of $ONOO^-$ decay in the presence or absence of the different types of LmPP proteins was measured by stopped-flow spectroscopy at 100 mM phosphate buffer (pH 6.0).[17,18,21] The rate of reactions was measured by following the decrease in absorbance changes at 340 nm instead of 302 nm due to the wavelength limitation of our stopped-flow spectrophotometer. The multiple-turnover number of $ONOO^-$ degradation is expressed in inverse seconds. Reactions were initiated by rapidly mixing 4.0 μM wild-type or mutant enzymes in the presence of 100 mM phosphate buffer (pH 6.0), with 400 μM peroxynitrite in 0.005 N NaOH. The molar extinction coefficient of $ONOO^-$ is 868 mM^{-1} cm^{-1} at 340 nm.

Imidazole Complex of the Wild Type and Mutants. The pH of the stock solution of imidazole was adjusted to 6.0 with HCl. Scans from 700 to 350 nm of wild-type LmPP and its mutants were taken before and after addition of 50 mM imidazole at room temperature in the presence of 50 mM potassium phosphate buffer (pH 6.0).

Formation of Fe^{II} Species of the Wild Type and Mutants. Ferric wild-type LmPP and its mutants in 50 mM Tris-HCl buffer (pH 8.8) were bubbled using nitrogen gas to remove any oxygen contamination to semianaerobic conditions, and a pinch of solid dithionite was added to the cuvette. Then samples were scanned from 350 to 700 nm at room temperature. Each set of experiments was conducted using freshly purified enzymes to prevent any change in the spin state due to the freezing, thawing, and storage of enzymes.

Spectra of the Fe^{II}−CO Complex of the Wild Type and Mutants. Ferric wild-type LmPP and its mutants were reduced to the ferrous state using a stoichiometric excess of dithionite, and CO gas was bubbled through a needle into the cuvette fit with an airtight syringe. Immediately a spectrophotometric scan from 700 to 350 nm was performed at room temperature on a Shimadzu-2550 UV−vis spectrophotometer. In each experiment, spectra of freshly purified enzymes were recorded in the presence of 50 mM Tris-HCl buffer (pH 8.8) or 50 mM phosphate (pH 4.0) at 25 °C.

Electron Paramagnetic Resonance Measurements. X-Band EPR spectra were recorded on a Jeol (JESFA200) apparatus. Spectra were recorded in 50 mM potassium phosphate at pH 4.0 for 0.2 mM LmPP and 50 mM potassium phosphate buffer at pH 6.0 for LmP.

RESULTS

Homology Modeling. On the basis of the homology model,[22,23] the structural features of LmPP are found to be similar to those of peanut peroxidase.[24] Taking advantage of the coordinates of the model, we have searched for the distal and proximal ligands that interact with the ferric heme iron of LmPP. Figure 1 depicts all cysteine and methionine residues of LmPP, distal glutamate 105, and the possible interactions between the heme iron and the proximal histidine 206 residue. Furthermore, the distances from proximal His206 and Cys205 residues from heme iron are 2.13 and 7.09 Å, respectively. In addition, the model structure predicts that the distances from distal Glu105 and the closest Cys107 residue to the heme iron are 5.96 and 16.05 Å, respectively.

Spectral Feature of Ferric Mutants. The optical spectra of wild-type LmPP showed the Soret peak at 423 nm with other peaks as the α band at 570 nm, the β band at 538 nm, and the δ band at 360 nm (Table 1). These types of spectral bands were characteristic of six-coordinate low-spin heme species with Cys ligated as reported for various heme proteins (Table 1).[25−27] Our spectroscopic analysis indicated that the replacement of Cys71, Cys199, Cys205, Cys268, Cys284, Met324, and Met120 with alanine did not alter the heme spin state, which closely resembled that of the wild type (Table 1), suggesting a lack of involvement of these residues in the formation of the ligand of the heme iron. In addition, a similar type of spectral band was observed with the replacement of Glu105 with leucine at the

dx.doi.org/10.1021/bi401343t | *Biochemistry* 2013, 52, 8878−8887

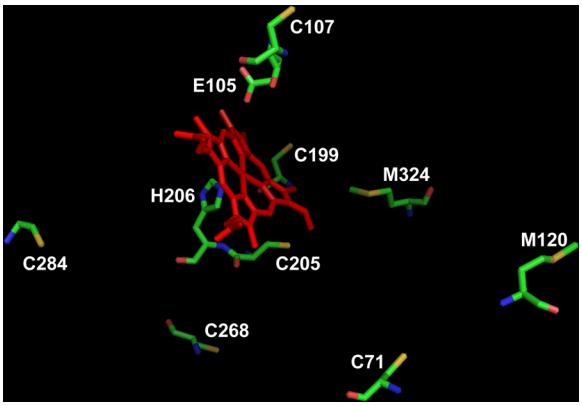

Figure 1. Structural model showing the positions of proximal histidine, distal glutamate, and all cysteine and methionine residues in LmPP. The amino acid residues of LmPP are numbered. On the basis of the published X-ray crystallographic structures of peanut peroxidase (Protein Data Bank entry 1sch), we constructed a three-dimensional model by homology modeling. Prediction of the three-dimensional structure of LmPP was conducted by knowledge-based homology modeling using the SWISS MODELWORKSPACE[22] and PyMOL.[59]

distal site. Interestingly, UV−visible spectra of the H206A and C205A/H206A mutants showed a blue shift of the Soret peak at 382 nm with the disappearance of the α band at 570 nm (shoulder) and the β band at 538 nm and the appearance of the CT1 band at 640 nm and the CT2 band at 515 nm (Table 1 and Figure 2). Earlier spectroscopic data of high-spin $P450_{CAM}$ and CPO showed Soret peaks at 391 and 396 nm with CT1 bands at 509 and 515 nm and CT2 bands at 646 and 650 nm, respectively.[28,29] These spectral peaks are characteristic of cysteine five-coordinate high-spin heme as reported for nitric oxide synthase, CPO, and $P450_{CAM}$.[28−30] On the other hand, the optical spectra of the C107A mutant showed a typical histidine five-coordinate high-spin heme with a Soret peak at 408 nm and corresponding charge transfer bands CT1 and CT2 at 527 and 630 nm, respectively (Table 1 and Figure 2).

The EPR spectra of wild-type LmPP and the E105L mutant show nearly identical sets of g values (2.56, 2.27, and 1.87 for the imidazole complex of the ferric P450 and 2.52, 2.28, and 1.88 for the ferric *Bx*RcoM2), which can be seen from Figure 3 and in Table 2. The ferric H206A mutant had a high-spin EPR signal (Figure 3; Table 2 for summary) analogous to the spectra of cysteine-ligated ferric $P450_{CAM}$ and CPO with g values in the range of 7−8.[31,32] In contrast, the ferric C107A mutant had a high-spin EPR signal (Figure 3; Table 2 for summary) analogous to the spectra of histidine-ligated ferric LmP with g values in the 5.78 region.

Figure 2 compares the electronic absorption spectra of ferric H206A, C205A, C205A/H206A, E105L, and C107A mutants at various pH values. The pH-dependent changes in the coordinates of H206A, C205A/H206A. and C107A mutants were observed in 50 mM phosphate buffer (pH 4.0 and 7.5). At pH 4.0, H206A, C205A/H206A. and C107A mutants included high-spin heme, whereas the wild type, C205A, and E105L included 6cLS derivatives. As the pH is increased to 7.5, H206A, C205A/H206A, and C107A mutants generated 6cLS derivatives; however, the electronic spectra of the mutants were different (α_{max} values for H206A and C205A/H206A of 380, 420, 540, 580, and 640 nm; α_{max} values for C107A of 417, 540, and 577 nm).

Sometimes external ligand imidazole can bind at position 6 in high-spin ferric heme and display distinguishable spectral features depending on whether the fifth ligand is a histidine

Table 1. Comparison of Absorption Peak Positions and (Milli)molar Absorptivity (mM^{-1} cm^{-1}) for Ferric Wild-Type LmPP, LmPP Mutants, and Other Heme Proteins

protein	ligands	δ	Soret	β	α	CT	ref
wild-type LmPP	His/Cys[a]	360 (29)	423 (69)	538 (5.8)	570 (4.6)	640 (0.6)	this work
C71A LmPP	His/Cys[a]	360 (29)	423 (69)	538 (5.8)	570 (4.6)	640 (0.6)	this work
M120A LmPP	His/Cys[a]	360 (29)	423 (69)	538 (5.8)	570 (4.6)	640 (0.6)	this work
C199A LmPP	His/Cys[a]	360 (29)	423 (69)	538 (5.8)	570 (4.6)	640 (0.6)	this work
C205A LmPP	His/Cys[a]	360 (32)	423 (71)	538(8.2)	570(6.1)	640(0.8)	this work
C268A LmPP	His/Cys[a]	360 (29)	423 (69)	538 (5.8)	570 (4.6)	640 (0.6)	this work
C284A LmPP	His/Cys[a]	360 (29)	423 (69)	538 (5.8)	570 (4.6)	640 (0.6)	this work
M324A LmPP	His/Cys[a]	360 (29)	423 (69)	538 (5.8)	570 (4.6)	640 (0.6)	this work
E105L LmPP	His/Cys[a]	360 (20)	423 (75)	538 (7.1)	570 (5.7)	640 (0.4)	this work
*Rr*CooA	Pro/Cys	362 (nr)	424 (nr)	540 (nr)	574 (nr)	649 (nr)	25
*Bx*RcoM-2	His/Cys	354 (nr)	423 (nr)	541 (nr)	565 (nr)	640 (nr)	46
hCBS	His/Cys	365 (nr)	428 (nr)	550 (nr)	ND	650 (nr)	27
H206A LmPP	Cys[a]	ND	382 (89)	ND	ND	515 (12), 641 (4.2)	this work
C205A/H206A LmPP	Cys[a]	ND	382 (93)	ND	ND	515 (15), 641 (5.5)	this work
P450 (HS)	Cys	ND	391 (nr)	ND	ND	509 (nr), 644 (nr)	28
H206A LmPP with ImH	ImH/Cys[a]	360 (25)	423 (67)	538 (6.0)	570 (4.7)	640 (0.5)	this work
C205A/H206A LmPP with ImH	ImH/Cys[a]	360 (23)	423 (70)	538 (5.6)	570 (4.3)	640 (0.6)	this work
$P450_{CAM}$ with ImH	ImH/Cys	358 (nr)	425 (nr)	542 (nr)	574 (nr)	638 (nr)	33
C107A LmPP	His[a]	ND	408 (89)	ND	ND	527 (12), 630 (5.1)	this work
LmP	His	ND	409 (nr)	ND	ND	502 (nr), 640 (nr)	38
C107A LmPP with ImH	His/ImH[a]	ND	413 (98)	534 (8.5)	565 (5.0)	ND	this work
LmP with ImH	His/ImH	ND	413 (nr)	537 (nr)	565 (nr)	ND	38

[a]Predicted axial ligand. Spectra of the ferric enzyme with and without the imidazole complex were assessed in the presence of 50 mM phosphate buffer at pH 6.0 and 4.0, respectively. ND and nr indicate not detected and not reported, respectively. The value of the millimolar extinction coefficient is given in parentheses.

dx.doi.org/10.1021/bi401343t | *Biochemistry* 2013, 52, 8878−8887

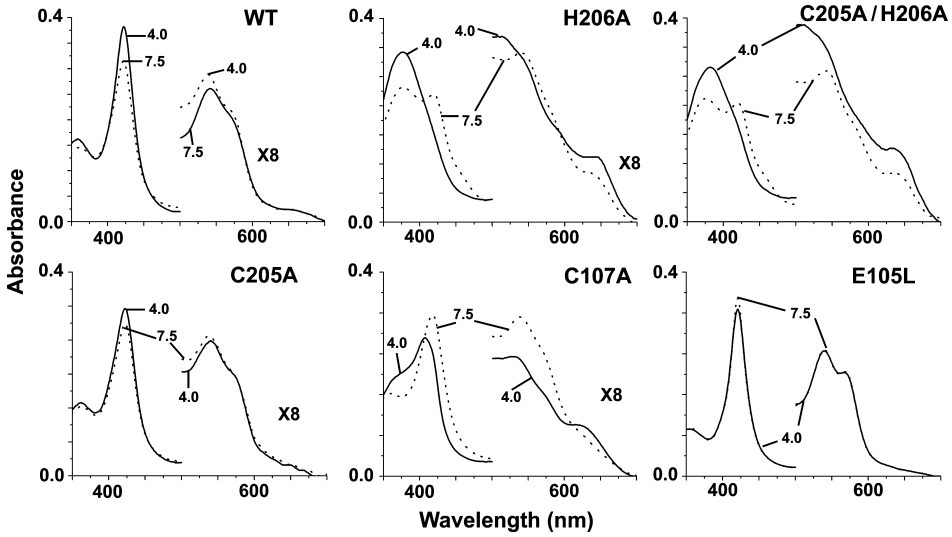

Figure 2. pH-dependent spectral studies of wild-type LmPP and its mutants. Wild-type and mutant enzymes were scanned in the presence of 50 mM phosphate buffer at pH 4.0 (···) and pH 7.5 (—). Visible regions were amplified 8-fold from 500 to 700 nm. Each spectrum is representative of three independent purifications in respective buffers. The concentrations of the wild type, E105L, C107A, C205A, H206A, and C205A/H206A were 5.8, 4.2, 3.2, 4.7, 3.8, and 3.4 μM, respectively.

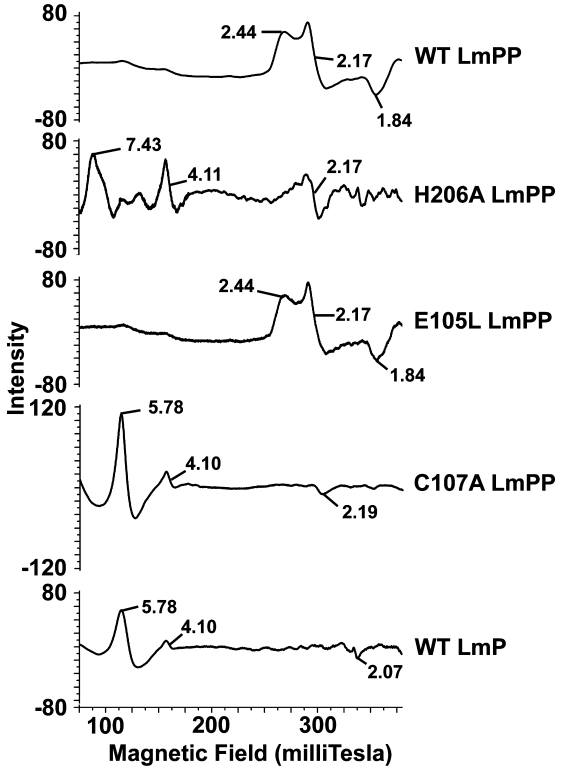

Figure 3. X-Band EPR spectra of 0.2 mM wild-type LmPP and its mutants in 50 mM phosphate (pH 4.0) containing 0.1 mM DTPA and X-band spectra of 0.2 mM wild-type LmP in 50 mM phosphate buffer (pH 6.0) containing 0.1 mM DTPA. The microwave power, modulation frequency, microwave frequency, and measurement temperature were 10 mW, 100 kHz, 9.1 GHz, and 77 K, respectively.

Table 2. X-Band EPR Parameters of Ferric Wild-Type LmPP, LmPP Mutants, and Other Heme Proteins

protein	ligands	g values	ref
wild-type LmPP	His/Cys[a]	2.44, 2.24, 1.84	this work
E105L LmPP	His/Cys[a]	2.44, 2.24, 1.84	this work
*Rr*CooA	Pro/Cys	2.46, 2.25, 1.89	10
*Bx*RcoM-2	His/Cys	2.52, 2.28, 1.88	46
hCBS	His/Cys	2.49, 2.31, 1.87	27
P450 (imidazole)	Cys/Imi	2.56, 2.27, 1.87	31
CPO (HS)	Cys	7.6, 4.3, 1.8	32
P450 (HS)	Cys	7.9, 4.0, 1.8	31
H206A LmPP	Cys[a]	7.43, 4.23, 2.3	this work
C107A LmPP	His[a]	5.78, 4.24, 2.19	this work
LmP	His	5.78, 4.23, 2.07	this work

[a]Predicted axial ligand.

or cysteine residue.[33,34] Therefore, we used imidazole to observe whether there was any change in Soret or visible peaks in the wild type and mutants. We found that the wild type, E105L, and C205A exhibited no changes in their spectral features at pH 6.0 in the presence of 50 mM imidazole, indicating that the fifth and sixth ligands were tightly bound with heme iron (Figure 4). The Soret maxima of H206A and C205A/H206A were red-shifted from 382 to 423 nm with an α band at 570 nm (shoulder) and a β band at 538 nm in the presence of 50 mM imidazole (Figure 4). These types of spectral changes occurred in cysteine five-coordinate ligated heme with external imidazole as reported for both nitric oxide synthase and cytochrome P450.[33,35] Similarly, the C107A mutant was a red-shifted from 408 to 412 nm with an α band at 565 nm (shoulder) and a β band at 535 nm via the addition of 50 mM imidazole (Figure 4), typical of bis(imidazole) ligation as in cytochrome b_5.[36,37] These types of spectral bands were characteristic of imidazole-bound histidine-ligated heme as reported for various histidine-ligated peroxidases.[38]

Another approach to study the heme iron ligation is by reduction of the ferric enzymes with dithionite at different pH values (acidic and alkaline). Like high-spin histidine-ligated heme proteins,[39,40] the Fe^{II} state of the wild type, C205A, C107A, and E105L displayed noticeable spectral features and showed a Soret peak at ~428 nm and a visible peak at 557 nm indicating that the ferrous state of these enzymes had a 5cHS heme at pH 8.8 (Figure 5 and Table 3). Interestingly, UV–visible spectra of the Fe^{II} state of H206A and C205A/H206A

dx.doi.org/10.1021/bi401343t | *Biochemistry* 2013, 52, 8878–8887

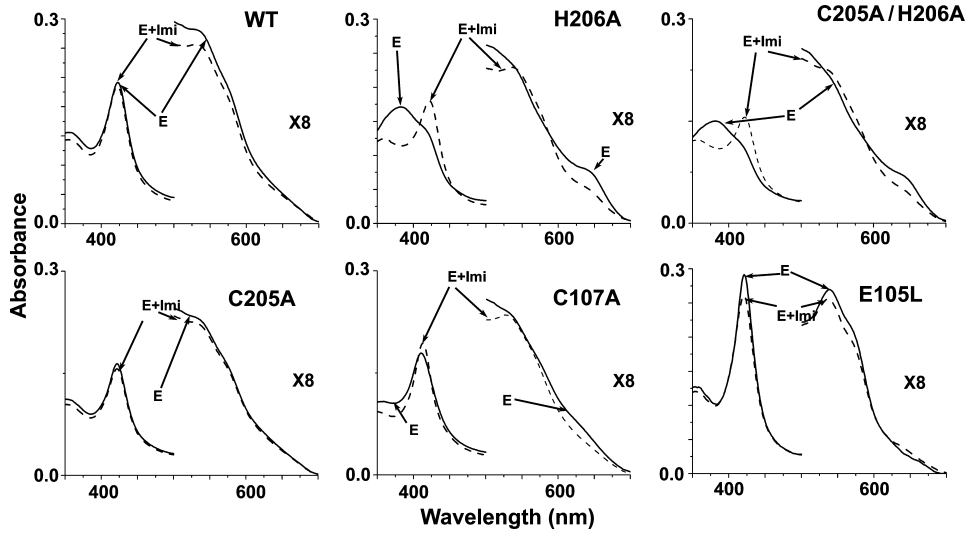

Figure 4. Soret and visible absorption spectra of the ferric wild type and mutants in the presence of 50 mM phosphate buffer (pH 6.0) with (---) or without (—) 50 mM imidazole. The concentrations of the wild type, E105L, C107A, C205A, H206A, and C205A/H206A were 2.9, 4.0, 2.2, 2.5, 2.3, and 2.0 μM, respectively.

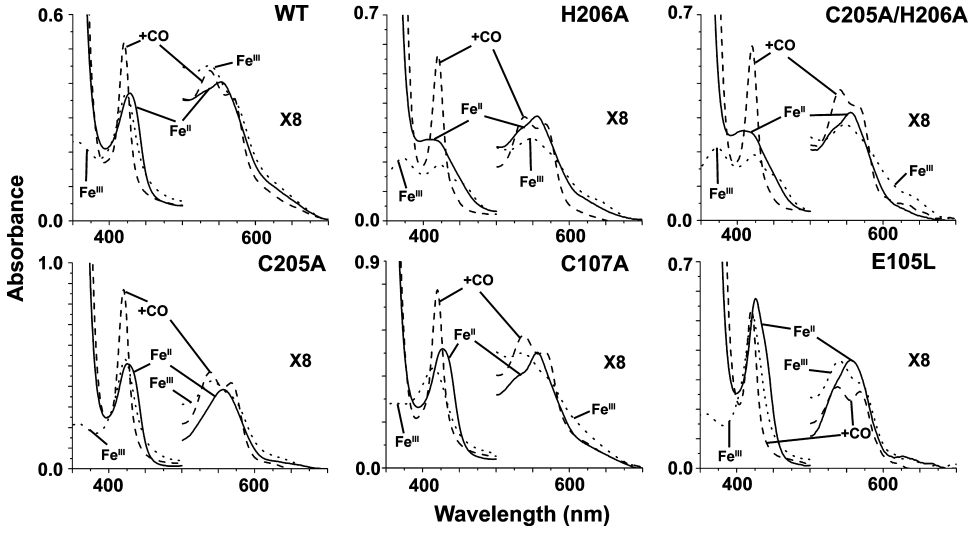

Figure 5. Fe^{II}- and CO-bound spectral characteristics of the wild type and mutants in 50 mM Tris-HCl buffer (pH 8.8). Ferric enzymes were reduced to Fe^{II} enzymes using solid dithionite, and ferrous enzymes were bubbled with CO to produce the Fe^{II}–CO complex. Each scan was representative of six independent experiments. The concentrations of the wild type, E105L, C107A, C205A, H206A, and C205A/H206A were 5.3, 7.0, 5.0, 7.5, 4.0, and 4.3 μM, respectively.

showed a Soret peak at 412 nm with the appearance of the $\alpha\beta$ band at 557 nm (Figure 5 and Table 3) indicating that the ferrous states of both mutants were 5cHS heme with cysteine ligated.[41] To authenticate these data by an alternative method, the ferrous states of heme proteins were treated in parallel with carbon monoxide.[42] When the ferrous–CO complexes of the wild type and all mutant proteins were studied, all exhibited spectroscopically identical Soret maxima at 420 nm, β bands at 540 nm, and α bands at 568 nm (Figure 5 and Table S2 of the Supporting Information). Although the axial ligand of both H206A and C205A/H206A (ferric or ferrous) was found to be cysteine, they exhibited a Soret peak around 420 nm with a β band at 540 nm and an α band at 568 nm (Figure 5), indicating that these mutants behaved like P420 rather than P450.[43,44]

At pH 4.0, both of the dithionite-treated C107A and E105L mutants showed Soret peaks at ~428 nm and visible peaks at 557 nm indicating that the heme irons of these enzymes were completely reduced (Figure 6, solid line). On the other hand, the hemes of the wild type and all mutant proteins (except for C107A and E105L) were only partially reduced at pH 4.0 as judged by the two visible $\alpha\beta$ bands in the visible region (539 and 568 nm) (Figure 6, solid line) that were very close to those (538 and 570 nm) of their ferric forms. It has been shown that the low-spin form of anionic ligand-ligated heme proteins is not quickly reduced with dithionite (for example, P450 2B4).[45] However, Figure 6 shows the formation of complete ferrous–CO complexes for all the wild-type and mutant LmPPs (dotted line) because CO might influence an equilibrium shift between the ferric and ferrous state of hemes to complete the ferrous state by forming the ferrous–CO complex.

We compared $ONOO^-$ scavenging activity among wild-type LmPP and its mutants by measuring their multiple-turnover rates in the presence of 100 mM phosphate buffer (pH 6.0). The $ONOO^-$ decomposing activities for the wild type, H206A,

dx.doi.org/10.1021/bi401343t | *Biochemistry* 2013, 52, 8878–8887

Table 3. Comparison of Soret, Visible Absorption Maxima (nanometers), and (Milli)molar Absorptivities (mM^{-1} cm^{-1}) for Ferrous Wild-Type LmPP, LmPP Mutants, and Other Heme Proteins[a]

ferrous enzyme	ligands	Soret	$\beta\alpha$	ref
wild-type LmPP	His[b]	428 (73)	557 (10)	this work
C71A LmPP	His[b]	428 (73)	557 (10)	this work
M120A LmPP	His[b]	428 (73)	557 (10)	this work
C199A LmPP	His[b]	428 (73)	557 (10)	this work
C205A LmPP	His[b]	428 (74)	557 (8.0)	this work
C268A LmPP	His[b]	428 (73)	557 (10)	this work
C284A LmPP	His[b]	428 (73)	557 (10)	this work
M324A LmPP	His[b]	428 (73)	557 (10)	this work
E105L LmPP	His[b]	428 (75)	557 (6.5)	this work
*Rr*CooA	His/Pro	425 (nr)	529 (nr), 559 (nr)	10
*Bx*RcoM-2	His/Met	425 (nr)	532 (nr), 562 (nr)	46
hCBS	His/Cys	448 (nr)	540 (nr), 570 (nr)	27
H206A LmPP	Cys[b]	412 (52)	557 (8.6)	this work
C205A/H206A LmPP	Cys[b]	412 (54)	557 (8.6)	this work
P450 (HS)	Cys	408 (nr)	560 (nr)	28
C107A LmPP	His[b]	428 (105)	557 (11)	this work
LmP	His	436 (nr)	559 (nr)	38

[a]The stable ferrous enzymes were obtained by addition of dithionite in the presence of 50 mM Tris-HCl buffer (pH 8.8). nr indicates not reported. [b]Predicted axial ligand. The value of the millimolar extinction coefficient is given in parentheses.

C205A/H206A, and C107A were 23 ± 2.0, 1.2 ± 0.1, 1.4 ± 0.08, and 37.4 ± 3.2 s^{-1}, respectively. The C107A mutant exhibited 1.5-fold higher activity than the wild-type enzyme, whereas the catalytic activities of both H206A and C205A/H206A mutants were much lower than that exhibited by the wild-type enzyme. This marked decrease in the activity of the wild type reflects the fact that the sixth thiolate ligand in LmPP might prevent interaction of $ONOO^-$ with the heme iron. The data of both H206A and C205A/H206A mutants suggested that either the proximal site of the heme was less accessible to $ONOO^-$ or the reactivity of the distal site thiolate bond containing LmPP with $ONOO^-$ was lower than that of wild-type LmPP.

DISCUSSION

The EPR spectrum of wild-type ferric LmPP shows a single rhombic EPR signal (*g* values of 2.46, 2.25, and 1.89),[17] with a *g* value anisotropy characteristic of LS thiolate-bound heme.[11] In addition, the optical absorption spectrum of wild-type LmPP is like that of the 6cLS thiolate-ligated heme protein.[10,46] However, we note that the ferrous−CO absorption band at ∼450 nm in the chloroperoxidase and the cytochrome P450, which originate from a thiolate ligand,[11] is not observed in the CO-bound ferrous wild-type LmPP spectra.[17] Thus, the following two possible axial ligand combinations have been proposed to explain the characteristics of optical spectral bands in ferric and CO-bound ferrous LmPP.

(i) Like *Rr*CooA,[10] the ferric heme iron of wild-type LmPP may be coordinated by cysteine (thiolate) (Cys205) at the proximal site and by the nitrogen of the distal site unknown residue. When the heme is reduced, the cysteine (thiolate) is replaced with a neighboring histidine (His206), which poises the protein for binding CO via replacement of the distal site residue. However, the C205A mutant exhibits electronic absorption spectra in its ferric, ferrous, and ferrous−CO forms that were indistinguishable from those of the wild-type protein (Table 1). These results can rule out the possibility of proximal ligand as a cysteine in the ferric state of LmPP. In contrast, H206A and C205A/H206A mutants show substantial

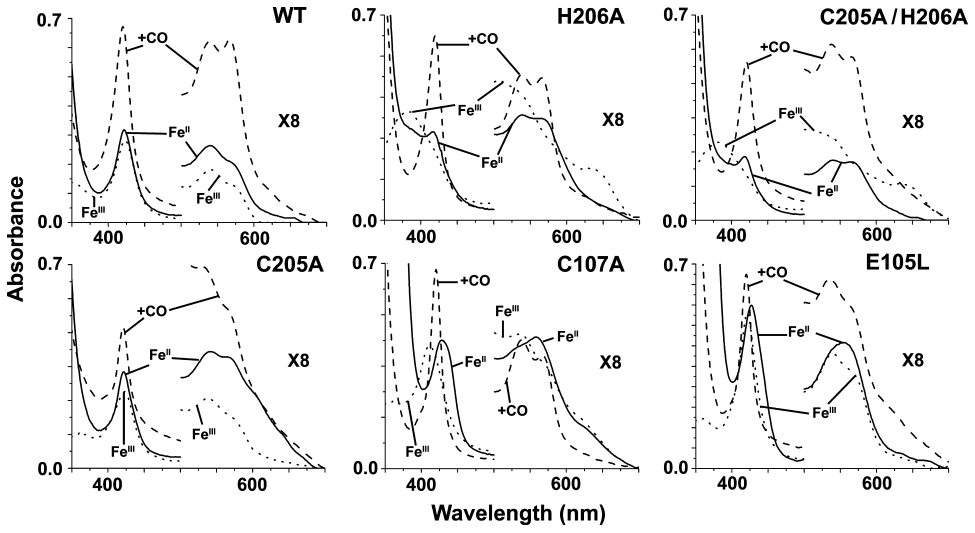

Figure 6. Fe^{II}- and CO-bound spectral characteristics of the wild type and mutants in 50 mM phosphate (pH 4.0). Ferric enzymes were reduced to Fe^{II} enzymes using solid dithionite, and ferrous enzymes were bubbled with CO to produce the Fe^{II}−CO complex. Each scan was representative of six independent experiments. The concentrations of the wild type, E105L, C107A, C205A, H206A, and C205A/H206A were 4.3, 7.0, 5.0, 4.3, 4.3, and 3.5 μM, respectively.

dx.doi.org/10.1021/bi401343t | *Biochemistry* 2013, 52, 8878−8887

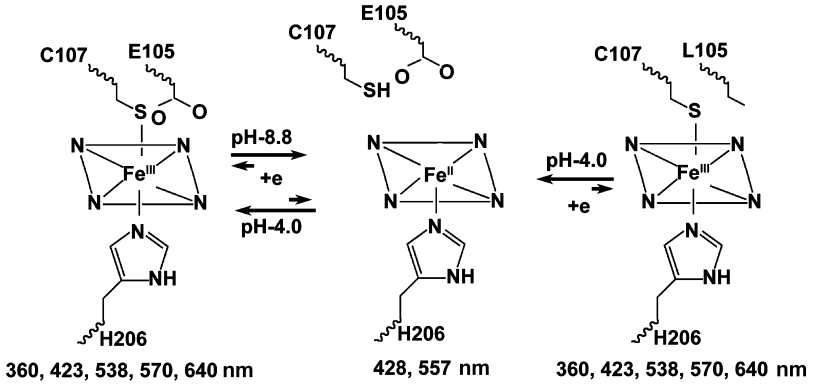

Figure 7. Possible schematic diagram for redox-dependent ligand switching in LmPP that explains the observed spectroscopic data of wild-type LmPP and its mutants.

changes in optical and EPR spectra compared to that of wild-type LmPP. The optical spectra of both H206A and C205A/H206A mutants are similar to those of high-spin cytochrome P450[28,33] and nitric oxide synthase,[47] indicating that thiolate ligation is retained in this variant at the distal site and suggesting that His206 is a ligand at the proximal site in the oxidized form of LmPP. Furthermore, the spectra of imidazole-bound H206A and C205A/H206A mutants are identical with those of the wild-type protein, providing further support for the thiolate/imidazole ligand assignment for ferric LmPP. Further evidence of stable cysteine ligation in the H206A mutant comes from the EPR spectrum of the high-spin state (Figure 3), which has a distinguishing characteristic of 5cHS ferric thiolate-bound heme proteins such as $P450_{CAM}$ or CPO displaying g values in the range of 7−8 (see Table 2).[32,48]

(ii) The heme in LmPP is unusual and resembles (but is also distinct from) that found in the hCBS.[49,50] Thus, the alternative possibility is that the ferric heme iron of wild-type LmPP is coordinated by the nitrogen of histidine (His206) at the proximal site and by the thiolate of the cysteine residue at the distal site. The proposed model structure based on molecular dynamics calculation and energy minimization cannot predict the possible distal site cysteine residue within 3 Å of heme iron. Except for the C107 mutant, all LmPP Cys and Met variants (C71A, C199A, C205A, C268A, C284A, M120A, and M324A) display normal amounts of heme-containing LmPP and exhibit electronic absorption spectra of the ferric, ferrous, and ferrous−CO forms that are identical to that of the wild-type protein (Table 1). In contrast, the C107A mutant shows a considerable amount of alteration in optical spectra compared to that of wild-type LmPP. The spectrum of the C107A mutant is similar to that of high-spin peroxidase,[51] indicating that histidine ligation is retained in this variant at the proximal site and suggesting that Cys107 is a ligand in the distal site in the oxidized form of LmPP. Further evidence of stable histidine ligation in the C107A mutant comes from the EPR spectrum of the high-spin state (Figure 3), which has a unique characteristic of 5cHS ferric histidine-bound heme proteins such as LmP, which displays g values of ∼6.0 (Table 2).

On the basis of mutational and spectroscopic analysis, our data presented in this study indicate that both His206 and Cys107 act as the axial ligands in the ferric state of the E105L mutant. Although the ferric state of the E105L mutant is identical with the ferric wild-type protein, a central question in this study is why the dithionite can be fully reduced in the E105L mutant but partially reduced in wild-type LmPP at acidic pH (Figure 6). The reason for such an extremely slow reduction of the heme iron of wild-type LmPP may be the lowered redox potentials of anionic ligand-ligated hemes versus those of neutral ligand-ligated hemes even though the observed factor appears to be more kinetics than equilibrium. The anionic residue (E105 in LmPPs) at the distal site of the heme iron might prevent the heme reduction at acidic pH. Thus, removal of C107 (heme axial anionic ligand) or E105 (anionic side chain) might eliminate such kinetic and equilibrium barriers for dithionite reduction of the heme. It is well-known that the formation of a complex of ferrous heme with an anionic thiolate ligand is usually not easy to achieve, although a ferric adduct with the same type of ligand can be obtained without any difficulty. This is mainly due to weakening of the heme iron−anionic ligand bond (i.e., charge repulsion) caused by an increased negative charge on iron upon reduction.[52,53] Only built-in systems in heme proteins such as a (multiple) H-bond(s) to the ligated anionic donor atom would support and stabilize thiolate−ferrous heme iron coordination.[54] High pH values would also help as is the case for alkaline cystathionine β-synthase.[27] Like hCBS,[50] the ferric heme iron of wild-type LmPP is coordinated by cysteine (thiolate) (Cys107) at the distal site and by the imidazole of the proximal site His206 residue, but the Soret band of ferrous wild-type LmPP (428 nm) is different from that of the ferrous state of hCBS (450 nm) at alkaline pH. One possibility is that, when the heme in wild-type LmPP is reduced, the cysteine (thiolate) distal bond may be broken and the subsequently reduced state of wild-type LmPP can display a high spin with histidine ligated. As seen for wild-type LmPP, earlier ligand switching is reported in many heme proteins that are cysteinate-bound in the ferric state and do not retain such coordination in the ferrous state, like the inactive P420 forms of P450s,[43] and the inactive C420 form of CPO,[44] the CO-sensing CooA protein,[10,55] proximal His-to-Cys mutants such as that of myoglobin,[56] the CCP mutant,[34] and heme oxygenase.[57]

We have conducted mutational studies in LmPP and have made a possible schematic diagram of axial ligands of ferric and ferrous forms (Figure 7). On the basis of our results, we propose that the resting state of Fe^{III} LmPP is low-spin and six-coordinate with His206/Cys107 axially coordinated, as illustrated in Figure 7. The Fe^{III} heme of LmPP is 6cLS with cysteine 107 (thiolate) as one of the ligands, and this cysteine (thiolate) is lost upon reduction. As seen previously for hCBS,[27] the pH dependence of the rate of Fe^{II} LmPP formation suggests that both an axial anionic ligand (C107) and an

dx.doi.org/10.1021/bi401343t | Biochemistry 2013, 52, 8878−8887

anionic residue (E105) within the distal site of heme are controlling the kinetic and equilibrium barriers for dithionite reduction of the heme. Thus, removal of any one of them might eliminate these barriers.

Finally, this study aimed to determine whether a link exists between the axial sixth ligand of heme iron and the $ONOO^-$ degrading activity in the physiological pH range. One possibility is that the axial distal ligand of the heme iron might regulate the $ONOO^-$ degrading activity through the displacement of its six-coordinate environment. Earlier metmyoglobin work demonstrated that a five-coordinate ferric heme (His-heme) structure is favored over a six-coordinate heme for catalytic peroxynitrite decomposition.[58] The behavior of $ONOO^-$ degrading activity in our LmPP mutants is very similar to that of earlier distal and proximal mutants of metmyoglobin.[58] Although the distal site axial ligand of LmPP prevents the $ONOO^-$ degrading activity, it cannot be determined why the six-coordinate low-spin heme coordination mode (His−heme−Cys) is present in this particular type of peroxynitrite scavenging pseudoperoxidase (LmPP).

■ ASSOCIATED CONTENT

Supporting Information

List of oligonucleotides for mutations (Table S1) and comparison of Soret and visible absorption maxima (nanometers) for CO-bound ferrous wild-type and mutant LmPP (Table S2). This material is available free of charge via the Internet at http://pubs.acs.org.

■ AUTHOR INFORMATION

Corresponding Author

*Telephone: +91 33 2473-6793. Fax: +91 33 2473 5197. E-mail: adaks@iicb.res.in.

Funding

This work was supported by Council of Scientific and Industrial Research (CSIR) Project BSC 0114, an ICMR fellowship to R.S., CSIR Fellowships to M.B., and CSIR-SPM Fellowships to S.S.S.

Notes

The authors declare no competing financial interest.

■ ABBREVIATIONS

EPR, electron paramagnetic resonance; LmPP, *Leishmania major* pseudoperoxidase; LmP, *L. major* peroxidase; HRP, horseradish peroxidase; CCP, cytochrome *c* peroxidase; NOS, nitric oxide synthase; $OONO^-$, peroxynitrite; *Rr*CooA, heme-containing CO-sensing transcriptional factor in *Rhodospirillum rubrum*; hCBS, human cystathionine *β*-synthase; $P450_{CAM}$, camphor-hydroxylating cytochrome P450 from *Pseudomonas putida*; CPO, chloroperoxidase from the mold *C. fumago*; *Bx*RcoM-2, transcription regulator RcoM-2 from *Burkholderia xenovorans*; 6cLS, six-coordinate low-spin; 5cHS, five-coordinate high-spin.

■ REFERENCES

(1) Sono, M., Roach, M. P., Coulter, E. D., and Dawson, J. H. (1996) Heme-Containing Oxygenases. *Chem. Rev. 96*, 2841−2887.

(2) Girvan, H. M., and Munro, A. W. (2013) Heme Sensor Proteins. *J. Biol. Chem. 288*, 13194−13203.

(3) Sun, J., Loehr, T. M., Wilks, A., and Ortiz de Montellano, P. R. (1994) Identification of histidine 25 as the heme ligand in human liver heme oxygenase. *Biochemistry 33*, 13734−13740.

(4) Dunford, H. B. (1999) *Heme peroxidases*, John Wiley & Sons, Inc., New York.

(5) Reid, T. J., III, Murthy, M. R., Sicignano, A., Tanaka, N., Musick, W. D., and Rossmann, M. G. (1981) Structure and heme environment of beef liver catalase at 2.5 Å resolution. *Proc. Natl. Acad. Sci. U.S.A. 78*, 4767−4771.

(6) Erman, J. E., Hager, L. P., and Sligar, S. G. (1994) Cytochrome P-450 and peroxidase chemistry. *Adv. Inorg. Biochem. 10*, 71−118.

(7) Lomonosova, E. E., Kirsch, M., Rauen, U., and Droot, H. D. (1998) The critical role of HEPES in SIN-1 cytotoxicity, peroxynitrite versus hydrogen peroxide. *Free Radical Biol. Med. 24*, 522−528.

(8) Sono, M., Stuehr, D. J., Ikeda-Saito, M., and Dawson, J. H. (1995) Identification of nitric oxide synthase as a thiolate-ligated heme protein using magnetic circular dichroism spectroscopy. Comparison with cytochrome P-450-CAM and chloroperoxidase. *J. Biol. Chem. 270*, 19943−19948.

(9) Ojha, S., Hwang, J., Kabil, O., Penner-Hahn, J. E., and Banerjee, R. (2000) Characterization of the heme in human cystathionine *β*-synthase by X-ray absorption and electron paramagnetic resonance spectroscopies. *Biochemistry 39*, 10542−10547.

(10) Shelver, D., Thorsteinsson, M. V., Kerby, R. L., Chung, S. Y., Roberts, G. P., Reynolds, M. F., Parks, R. B., and Burstyn, J. N. (1999) Identification of two important heme site residues (cysteine 75 and histidine 77) in CooA, the CO-sensing transcription factor of *Rhodospirillum rubrum*. *Biochemistry 38*, 2669−2678.

(11) Reynolds, M. F., Shelver, D., Kerby, R. L., Parks, R. B., Roberts, G. P., and Burstyn, J. N. (1998) EPR and electronic absorption spectroscopies of the CO-sensing CooA protein reveal a cysteine-ligated low-spin ferric heme. *J. Am. Chem. Soc. 120*, 9080−9081.

(12) Omura, T., Sadano, H., Hasegawa, T., Yoshida, Y., and Kominami, S. (1984) Hemoprotein H-450 identified as a form of cytochrome P-450 having an endogenous ligand at the 6th coordination position of the heme. *J. Biochem. 96*, 1491−1500.

(13) Green, E. L., Taoka, S., Banerjee, R., and Loehr, T. M. (2001) Resonance Raman characterization of the heme cofactor in cystathionine *β*-synthase. Identification of the Fe-S(Cys) vibration in the six-coordinate low-spin heme. *Biochemistry 40*, 459−463.

(14) Aono, S., Ohkubo, K., Matsuo, T., and Nakajima, H. (1998) Redox-controlled ligand exchange of the heme in the CO-sensing transcriptional activator CooA. *J. Biol. Chem. 273*, 25757−25764.

(15) Lanzilotta, W. N., Schuller, D. J., Thorsteinsson, M. V., Kerby, R. L., Roberts, G. P., and Poulos, T. L. (2000) Structure of the CO sensing transcription activator CooA. *Nat. Struct. Biol. 7*, 876−880.

(16) Thorsteinsson, M. V., Kerby, R. L., Conrad, M., Youn, H., Staples, C. R., Lanzilotta, W. N., Poulos, T. J., Serate, J., and Roberts, G. P. (2000) Characterization of variants altered at the N-terminal proline, a novel heme-axial ligand in CooA, the CO-sensing transcriptional activator. *J. Biol. Chem. 275*, 39332−39338.

(17) Bose, M., Saha, R., Sen Santara, S., Mukherjee, S., Roy, J., and Adak, S. (2012) Protection against peroxynitrite by pseudoperoxidase from Leishmania major. *Free Radical Biol. Med. 53*, 1819−1828.

(18) Saha, R., Bose, M., and Adak, S. (2013) Mutation of Val90 to His in the pseudoperoxidase from *Leishmania major* enhances peroxidase activity. *Biochim. Biophys. Acta 1834*, 651−657.

(19) Yadav, R. K., Dolai, S., Pal, S., and Adak, S. (2008) Role of tryptophan-208 residue in cytochrome c oxidation by ascorbate peroxidase from *Leishmania major*: Kinetic studies on Trp208Phe mutant and wild type enzyme. *Biochim. Biophys. Acta 1784*, 863−871.

(20) Yadav, R. K., Pal, S., Dolai, S., and Adak, S. (2011) Role of proximal methionine residues in *Leishmania major* peroxidase. *Arch. Biochem. Biophys. 515*, 21−27.

(21) Saha, R., Bose, M., Santara, S. S., Roy, J., Yadav, R. K., and Adak, S. (2013) Effect of distal His mutation on the peroxynitrite reactivity of *Leishmania major* peroxidase. *Biochim. Biophys. Acta 1834*, 2057.

(22) Schwede, T., Kopp, J., Guex, N., and Peitsch, M. C. (2003) SWISS-MODEL: An automated protein homology-modeling server. *Nucleic Acids Res. 31*, 3381−3385.

(23) Arnold, K., Bordoli, L., Kopp, J., and Schwede, T. (2006) The SWISS-MODEL workspace: A web-based environment for protein structure homology modelling. *Bioinformatics 22*, 195−201.
(24) Schuller, D. J., Ban, N., Huystee, R. B., McPherson, A., and Poulos, T. L. (1996) The crystal structure of peanut peroxidase. *Structure 4*, 311−321.
(25) Clark, R. W., Youn, H., Parks, R. B., Cherney, M. M., Roberts, G. P., and Burstyn, J. N. (2004) Investigation of the role of the N-terminal proline, the distal heme ligand in the CO sensor CooA. *Biochemistry 43*, 14149−14160.
(26) Lu, Y., Casimiro, D. R., Bren, K. L., Richards, J. H., and Gray, H. B. (1993) Structurally engineered cytochromes with unusual ligand-binding properties: Expression of *Saccharomyces cerevisiae* Met-80 → Ala iso-1-cytochrome c. *Proc. Natl. Acad. Sci. U.S.A. 90*, 11456−11459.
(27) Pazicni, S., Lukat-Rodgers, G. S., Oliveriusova, J., Rees, K. A., Parks, R. B., Clark, R. W., Rodgers, K. R., Kraus, J. P., and Burstyn, J. N. (2004) The redox behavior of the heme in cystathionine β-synthase is sensitive to pH. *Biochemistry 43*, 14684−14695.
(28) Yu, C., Gunsalus, I. C., Katagiri, M., Suhara, K., and Takemori, S. (1974) Cytochrome P-450cam. I. Crystallization and properties. *J. Biol. Chem. 249*, 94−101.
(29) Hollenberg, P. F., and Hager, L. P. (1973) The P-450 nature of the carbon monoxide complex of ferrous chloroperoxidase. *J. Biol. Chem. 248*, 2630−2633.
(30) White, K. A., and Marletta, M. A. (1992) Nitric oxide synthase is a cytochrome P-450 type hemoprotein. *Biochemistry 31*, 6627−6631.
(31) Lipscomb, J. D. (1980) Electron paramagnetic resonance detectable states of cytochrome P-450cam. *Biochemistry 19*, 3590−3599.
(32) Hollenberg, P. F., Hager, L. P., Blumberg, W. E., and Peisach, J. (1980) An electron paramagnetic resonance study of the high and low spin forms of chloroperoxidase. *J. Biol. Chem. 255*, 4801−4807.
(33) Dawson, J. H., Andersson, L. A., and Sono, M. (1982) Spectroscopic investigations of ferric cytochrome P-450-CAM ligand complexes. Identification of the ligand trans to cysteinate in the native enzyme. *J. Biol. Chem. 257*, 3606−3617.
(34) Sigman, J. A., Pond, A. E., Dawson, J. H., and Lu, Y. (1999) Engineering cytochrome c peroxidase into cytochrome P450: A proximal effect on heme-thiolate ligation. *Biochemistry 38*, 11122−11129.
(35) Sennequier, N., Wolan, D., and Stuehr, D. J. (1999) Antifungal imidazoles block assembly of inducible NO synthase into an active dimer. *J. Biol. Chem. 274*, 930−938.
(36) Ozols, J., and Strittmatter, P. (1964) The Interaction of Porphyrins and Metalloporhyrins with Apocytochrome β-5. *J. Biol. Chem. 239*, 1018−1023.
(37) Mukherjee, S., Sen Santara, S., Das, S., Bose, M., Roy, J., and Adak, S. (2012) NAD(P)H cytochrome b5 oxidoreductase deficiency in *Leishmania major* results in impaired linoleate synthesis followed by increased oxidative stress and cell death. *J. Biol. Chem. 287*, 34992−35003.
(38) Yadav, R. K., Dolai, S., Pal, S., and Adak, S. (2010) Role of C-terminal acidic cluster in stabilization of heme spin state of ascorbate peroxidase from *Leishmania major*. *Arch. Biochem. Biophys. 495*, 129−135.
(39) Keilin, D., and Hartree, E. F. (1951) Purification of horse-radish peroxidase and comparison of its properties with those of catalase and methaemoglobin. *Biochem. J. 49*, 88−104.
(40) Han, S., Rousseau, D. L., Giacometti, G., and Brunori, M. (1990) Metastable intermediates in myoglobin at low pH. *Proc. Natl. Acad. Sci. U.S.A. 87*, 205−209.
(41) Dawson, J. H., Andersson, L. A., and Sono, M. (1983) The diverse spectroscopic properties of ferrous cytochrome P-450-CAM ligand complexes. *J. Biol. Chem. 258*, 13637−13645.
(42) Iizuka, T., Makino, R., Ishimura, Y., and Yonetani, T. (1985) Reversible acidic-alkaline transition of the carbon monoxide complex of cytochrome c peroxidase. *J. Biol. Chem. 260*, 1407−1412.
(43) Martinis, S. A., Blanke, S. R., Hager, L. P., Sligar, S. G., Hoa, G. H., Rux, J. J., and Dawson, J. H. (1996) Probing the heme iron coordination structure of pressure-induced cytochrome P420cam. *Biochemistry 35*, 14530−14536.
(44) Blanke, S. R., Martinis, S. A., Sligar, S. G., Hager, L. P., Rux, J. J., and Dawson, J. H. (1996) Probing the heme iron coordination structure of alkaline chloroperoxidase. *Biochemistry 35*, 14537−14543.
(45) Perera, R., Sono, M., Kinloch, R., Zhang, H., Tarasev, M., Im, S. C., Waskell, L., and Dawson, J. H. (2011) Stabilization and spectroscopic characterization of the dioxygen complex of wild-type cytochrome P4502B4 (CYP2B4) and its distal side E301Q, T302A and proximal side F429H mutants at subzero temperatures. *Biochim. Biophys. Acta 1814*, 69.
(46) Marvin, K. A., Kerby, R. L., Youn, H., Roberts, G. P., and Burstyn, J. N. (2008) The transcription regulator RcoM-2 from *Burkholderia xenovorans* is a cysteine-ligated hemoprotein that undergoes a redox-mediated ligand switch. *Biochemistry 47*, 9016−9028.
(47) Stuehr, D. J., and Ikeda-Saito, M. (1992) Spectral characterization of brain and macrophage nitric oxide synthases. Cytochrome P-450-like hemeproteins that contain a flavin semiquinone radical. *J. Biol. Chem. 267*, 20547−20550.
(48) Tsai, R., Yu, C. A., Gunsalus, I. C., Peisach, J., Blumberg, W., Orme-Johnson, W. H., and Beinert, H. (1970) Spin-state changes in cytochrome P-450cam on binding of specific substrates. *Proc. Natl. Acad. Sci. U.S.A. 66*, 1157−1163.
(49) Taoka, S., West, M., and Banerjee, R. (1999) Characterization of the heme and pyridoxal phosphate cofactors of human cystathionine β-synthase reveals nonequivalent active sites. *Biochemistry 38*, 2738−2744.
(50) Taoka, S., and Banerjee, R. (2001) Characterization of NO binding to human cystathionine β-synthase: Possible implications of the effects of CO and NO binding to the human enzyme. *J. Inorg. Biochem. 87*, 245−251.
(51) Adak, S., and Datta, A. K. (2005) *Leishmania major* encodes an unusual peroxidase that is a close homologue of plant ascorbate peroxidase: A novel role of the transmembrane domain. *Biochem. J. 390*, 465−474.
(52) Adachi, S., Nagano, S., Ishimori, K., Watanabe, Y., Morishima, I., Egawa, T., Kitagawa, T., and Makino, R. (1993) Roles of proximal ligand in heme proteins: Replacement of proximal histidine of human myoglobin with cysteine and tyrosine by site-directed mutagenesis as models for P-450, chloroperoxidase, and catalase. *Biochemistry 32*, 241−252.
(53) Egeberg, K. D., Springer, B. A., Martinis, S. A., Sligar, S. G., Morikis, D., and Champion, P. M. (1990) Alteration of sperm whale myoglobin heme axial ligation by site-directed mutagenesis. *Biochemistry 29*, 9783−9791.
(54) Perera, R., Sono, M., Voegtle, H. L., and Dawson, J. H. (2011) Molecular basis for the inability of an oxygen atom donor ligand to replace the natural sulfur donor heme axial ligand in cytochrome P450 catalysis. Spectroscopic characterization of the Cys436Ser CYP2B4 mutant. *Arch. Biochem. Biophys. 507*, 119.
(55) Nakajima, H., Nakagawa, E., Kobayashi, K., Tagawa, S., and Aono, S. (2001) Ligand-switching intermediates for the CO-sensing transcriptional activator CooA measured by pulse radiolysis. *J. Biol. Chem. 276*, 37895−37899.
(56) Hildebrand, D. P., Ferrer, J. C., Tang, H. L., Smith, M., and Mauk, A. G. (1995) Trans effects on cysteine ligation in the proximal His93Cys variant of horse heart myoglobin. *Biochemistry 34*, 11598−11605.
(57) Liu, Y., Moenne-Loccoz, P., Hildebrand, D. P., Wilks, A., Loehr, T. M., Mauk, A. G., and Ortiz de Montellano, P. R. (1999) Replacement of the proximal histidine iron ligand by a cysteine or tyrosine converts heme oxygenase to an oxidase. *Biochemistry 38*, 3733−3743.
(58) Herold, S., Kalinga, S., Matsui, T., and Watanabe, Y. (2004) Mechanistic studies of the isomerization of peroxynitrite to nitrate catalyzed by distal histidine metmyoglobin mutants. *J. Am. Chem. Soc. 126*, 6945.

(59) DeLano, W. L. (2002) *The PyMOL molecular graphics system*, DeLano Scientific, San Carlos, CA.